Acta Pharmaceutica Sinica B 2019;9(1):87–96

Chinese Pharmaceutical Association
Institute of Materia Medica, Chinese Academy of Medical Sciences

Acta Pharmaceutica Sinica B

www.elsevier.com/locate/apsb
www.sciencedirect.com

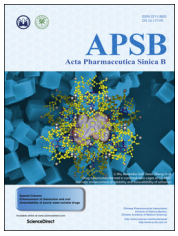

ORIGINAL ARTICLE

Intestinal uptake of barley protein-based nanoparticles for β-carotene delivery ☆

Guangyu Liu[†], **Ying Zhou**[†], **Lingyun Chen**[*]

Department of Agricultural, Food and Nutritional Science, University of Alberta, Alberta T6G 2P5, Canada

Received 13 June 2018; received in revised form 16 August 2018; accepted 22 August 2018

KEY WORDS

Barley protein;
Nanoparticles;
Hydrophobic;
Caco-2 cell;
Intestinal transport

Abstract Our previous study introduced a barley protein microparticle for encapsulation of hydrophobic drug/nutraceutical, which could release nanoparticles upon gastric digestion and deliver encapsulated compound to a simulated intestinal environment intact. This work focused on evaluating the potential of liberated nanoparticles to improve the absorption of encapsulated compounds (*e.g.*, β-carotene) using *in vitro* Caco-2 cell and *ex vivo* small intestine models. Nanoparticles obtained from gastric digestion of barley protein microparticles had a spherical shape and an average size of 351 nm. Nanoparticles showed low cytotoxicity in Caco-2 cells and their cellular uptake was dependent on time, concentration and temperature. In a Caco-2 cell monolayer model, significantly greater uptake and transport of β-carotene were observed when it was delivered by nanoparticles (15%), compared to free β-carotene suspension (2.6%). In an *ex vivo* rat jejunum model, nanoparticles showed the capacity to retain in small intestinal tissue. Approximately 2.24 and 6.04 μg nanoparticle were able to permeate through each cm^2 intestinal tissue and translocate to the serosal side after 60 and 90 min, respectively. Results from this study demonstrated the absorption improving effect of the barley protein nanoparticles and suggested their potential as vehicles for hydrophobic compounds.

[*]Corresponding author. Tel.: +1 780 492 0038.
E-mail address: lingyun.chen@ualberta.ca (Lingyun Chen).
[†]These authors made equal contributions to this work.
☆Invited for Special Column.
Peer review under responsibility of Institute of Materia Medica, Chinese Academy of Medical Sciences and Chinese Pharmaceutical Association.

https://doi.org/10.1016/j.apsb.2018.10.002

1. Introduction

Oral ingestion of drug is the most preferred route for drug delivery because of its convenience and high patient compliance. However, the bioavailability of many orally administered drugs can be compromised due to their poor solubility and/or low permeability in gastrointestinal tract[1,2]. Encapsulation of these drugs in nanoparticle carriers is one of the most promising strategies to improve their bioavailability due to the unique physicochemical properties of nanomaterials. The mechanisms by which this occurs involve increasing solubility of hydrophobic ingredients, protecting drugs from degradation in gastrointestinal environment, prolonging retention time against intestinal clearance mechanism, direct uptake of nanoparticles and eliminating first pass effect[3].

Proteins have excellent gelation, foaming and emulsification properties, which provide opportunities to make protein based nanoparticles for hydrophobic drug delivery[4–6]. Moreover, protein based nanoparticles showed many advantageous characteristics, like controlled release behavior[7], mucoadhesive property[8], enhanced intestinal permeability[9], which potentially enhance the absorption of orally administered drug.

Microparticles based on barley protein have been developed in our group by an emulsification–homogenization process[10]. Microparticles exhibited high encapsulation efficiency (over 92%) and loading efficiency (46.5%–50.1%) for hydrophobic compounds. They could also protect encapsulated compounds from environment stress (like oxidation) during storage, leading to increased shelf life. More interestingly, research found that nanoparticles were liberated from barley protein microparticle bulk matrix after enzymatic digestion in simulated gastric environment[11]. Such nanoparticles could resist gastric digestion and delivery encapsulated compounds to intestine intact for absorption, which provide a new strategy for controlled delivery of nanoparticles in the human gut. The *in situ* synthesis of nanoparticles in stomach also prevent nanoparticles from aggregation and degradation during storage. Nevertheless, information regarding the biological effects of the liberated nanoparticles remains unclear. This research aimed to investigate the potential of such nanoparticles to improve the absorption of encapsulated compounds using *in vitro* Caco-2 cell and *ex vivo* small intestine models. Nile red and β-carotene were used as indicators to evaluate the performance of nanoparticles. Nile red is a hydrophobic fluorescent dye which has been widely used in cell imaging to study the nanoparticle-cell interactions[12–15]. β-Carotene has numerous biological functions including antioxidant activity, prevention of cancer, heart disease and ocular disorders, and provitamin A activity[16,17]. Low stability and poor bioaccessibility represent two major challenges in the application of β-carotene. β-Carotene is unstable in the present of light, heat, and oxygen[17]. Barley protein microencapsulation can insulate encapsulated compounds from outside environment[10] therefore could increase the stability of β-carotene. The poor bioaccessibility of β-carotene is mainly attributed to its low solubility in aqueous environment[18,19]. Nanoparticle encapsulation can improve the bioaccessibility of β-carotene by increasing its dispersibility. The direct uptake of nanoparticles by intestine can also potentially enhance the absorption of β-carotene[20].

In this study, nanoparticles were prepared in a simulated gastric fluid by proteolysis of barley protein microparticles with pepsin. Then the effects of temperature, time and nanoparticle concentration on nanoparticle uptake were systematically investigated using Caco-2 cells. The permeability of nanoparticles was further explored using Caco-2 cell monolayers and rat jejunum tissues. Positive results will provide justification for further research effort to test *in vivo* efficacy of barley protein-based nanoparticles.

2. Materials and methods

2.1. Materials

Barley grain (Falcon) was provided by Dr. James Helm, Alberta Agricultural and Rural Development, Lacombe, Alberta. Human colorectal adenocarcinoma cell line Caco-2 was purchased from American Type Culture Collection (ATCC, Manassas, VA, USA). Cell culture reagents including Dulbecco's modified Eagle's medium (DMEM), fetal bovine serum (FBS), non-essential amino acids (NEAA), HEPES solution, trypsin-EDTA, Hank's balanced salt solution (HBSS), Dulbecco's phosphate-buffered saline (DPBS), phosphate buffered saline (PBS), Alexa Fluor dyes, DAPI and mounting medium were from Life Technologies (Burlington, ON). Cell culture flasks and multi-well plates were purchased from Corning (Tewksbury, MA, USA). Pepsin, Nile red and β-carotene were from Sigma–Aldrich (St. Louis, MO, USA). All other reagents and chemicals were purchased from Fisher Scientific (Waltham, MA, USA).

2.2. Preparation of nanoparticles

Barley protein microparticles (BMPs) were prepared using a high pressure homogenizing method reported by Wang et al.[10] Briefly, barley protein (hordeins:glutelins = 1:1) was dispersed in water at a percentage of 15% (*w/v*). A coarse emulsion was prepared by mixing barley protein dispersant with canola oil at the protein/oil ratio of 1:1 using a homogenizer (30,000 rpm, PowerGen 1000, Fisher Scientific Inc., CA, USA). Microparticles were then formed by passing the coarse emulsion through a high pressure homogenizer operated at 5000 psi (NanoDeBee, BEE International, Inc., MA, USA). Nile red-labeled BMPs and β-carotene-loaded BMPs were prepared by using canola oil dissolved with 0.025% (*w/v*) Nile red and 0.14% (*w/v*) β-carotene following the same procedure above.

2.3. In vitro digestion of microparticles

Nanoparticles (BNPs) were freshly prepared from BMPs before experiments[11]. Briefly, BMP dispersion was diluted to 10 mg/mL with acidic phosphate buffer (pH 2.0) and incubated with pepsin (1 mg/mL) at 37 °C for 15 min. The reaction was terminated by boiling the mixture for 5 min in water bath and then pH was adjusted back to 7 using 1 mol/L NaOH. Nile red-labeled BNPs (NR-NPs) and β-carotene loaded nanoparticles (BC-NPs) were prepared by using Nile red-labeled BMPs and β-carotene loaded BMPs following the same procedure above.

2.4. Characterization of nanoparticles

The size, size distribution (PdI), and zeta potential of BNPs were measured by dynamic light scattering using a zetasizer (Nano-ZS, Malvern Instruments Ltd., UK) at room temperature (22 °C). The refractive index of the nanoparticle and dispersion medium was set at 1.45 and 1.33, respectively. For size determination, BNPs were diluted to an appropriate concentration using distilled water to

avoid multiple scattering. For zeta potential determination, BNPs were diluted with phosphate buffer solution (10 mmol/L, pH 7) before measurement. The morphology of nanoparticles was examined by transmission electron microscopy (TEM). Briefly, one drop of BNP dispersion was placed onto a 300-mesh copper grid coated with carbon and let stand for 5 min. Then the excess water was removed by gently tapping filter paper at the edge of the grid without disturbing the surface. The grid was then stained with phosphotungstate (PTA) for 30 s and examined under Philips-FEI transmission electron microscope (Morgagni 268, FEI Co., Hillsboro, OR, USA) operated at 80 kV.

The encapsulation efficiency (EE) and loading capacity (LC) of β-carotene-loaded BNPs were determined by the equations below. For total β-carotene quantification, 1 mL BNP dispersant was mixed with 3 mL ethanol, sonicated for 15 min and extracted twice with hexane (4 mL). The hexane was then pooled and evaporated under nitrogen stream with β-carotene residue left in the vial. For free β-carotene quantification, 1 mL BNPs dispersant was mixed with 3 mL phosphate buffer solution (0.1 mol/L, with 0.9% NaCl, pH 5), and followed by centrifugation ($4000 \times g$, 15 min) to separate BNPs from aqueous phase. The free β-carotene in aqueous phase was then extracted with hexane and dried. The extracted residues were reconstituted with 300 µL acetonitrile/ethanol (v/v = 65/35) and analyzed using the method described in Section 2.8.

$$\text{EE}\ (\%) = \left(1 - \frac{\text{Free}\ \beta\text{-carotene}}{\text{Total}\ \beta\text{-carotene}}\right) \times 100 \quad (1)$$

$$\text{LC}\ (\%) = \frac{\text{Mass of}\ \beta\text{-carotene in BNPs}}{\text{Mass of BNPs}} \times 100 \quad (2)$$

2.5. Cell culture

Human colon carcinoma cell line Caco-2 was cultured in T-75 flasks at 37 °C in a humidified atmosphere of 95% air and 5% CO_2. High glucose (4500 mg/L) DMEM with sodium pyruvate (110 mg/L) and L-glutamin was used with supplementation of 20% FBS (v/v), 1% NEAA and 25 mmol/L HEPES. The medium was changed every other day and the cell morphology was monitored. Upon reaching 80% confluence, cells were detached with 0.25% trypsin in 1 mmol/L EDTA solution, gently centrifuged, resuspended and transferred to new flasks. Cells between passage 30 and 50 were used for experiments.

2.6. Cytotoxicity assay

The cytotoxicity of BNPs was examined by simultaneous staining with fluorescein diacetate (FDA) and propidium iodide (PI)[21–23]. Caco-2 cells were seeded onto 24-well plates at a density of 2.4×10^4 cells per well. After allowing the cells to grow for 24 h for attachment, BNPs were added to each well at sublethal concentrations and incubated with cells for 20 h. Upon removal of BNPs, cells were stained (8 µg/mL FDA and 20 µg/mL PI in PBS) and observed using a confocal laser scanning microscopy (CLSM, 510 Meta, Carl Zeiss, Jena, Germany). The living/dead cells in 3 fields (>300 cells) were counted in each well and the experiment was conducted in triplicate. Cell viability was expressed by the percentage of living cells in the test wells as a ratio to living cells in the control wells.

2.7. In vitro uptake study

2.7.1. Confocal laser scanning microscopy

The uptake of the nanoparticles was firstly studied using CLSM. Cells were seeded onto glass bottom microwell dishes (P35G-1.5-14-C, MatTek Corp., USA) at the density of 1×10^5 cells per dish and cultured for 5–7 days until reaching full confluency. On the day of experiment, the medium was replaced with HBSS (supplemented with 25 mmol/L HEPES, without phenol red) and cells were allowed to equilibrate at 37 °C for 30 min. Then HBSS was replaced with NR-NP dispersion (0.02 and 0.2 mg/mL in HBSS) and incubated with the cells for 0.5–6 h at 37 and 4 °C. At each endpoint, cells were gently rinsed with HBSS 3 times and fixed with 4% paraformaldehyde for 15 min at 37 °C. The cell membrane and nuclei were stained with WGA-Alexa Flour 488 conjugate and DAPI, respectively. Cells were further mounted with Prolong Gold Antifade Reagent, sealed with coverslips and observed using CLSM. Images were processed with ZEN 2009LE software (Carl Zeiss MicroImgaing GmbH, Germany).

2.7.2. Flow cytometry

The uptake of nanoparticle was further quantified by flow cytometry. Cells were seeded onto 6-well plates at the density of 1×10^5 cells per well and cultured for 5–7 days until reached a confluent monolayer. The cells were incubated with NR-NP dispersion at various concentration for 0.5–6 h at 37 and 4 °C. At each endpoint, cells were trypsinized, washed and resuspended in DPBS. The fluorescence associated with cells was measured with a flow cytometer (B.D. Biosciences FACSort, CA, USA) using FL2 detector at the wavelength of 580 nm. 10,000 cells were analyzed for each sample and mean fluorescence intensity (MFI) was evaluated.

In order to understand the uptake mechanism, three inhibitors, chlorpromazine hydrochloride (CPZ, 5 µg/mL), filipin III (FLI, 5 µg/mL) and cytochalasin D (CyD, 10 µg/mL) were used[24]. The cells were incubated with different inhibitors for 30 min then treated with NR-NP dispersion (0.2 mg/mL) by the same method mentioned above. The change of MFI at 2 h suggested possible uptake pathways.

2.8. In vitro transport efficiency study

Nanoparticles used in transport study were further processed using an *in vitro* digestion model[25]. Briefly, BC-NPs were equilibrated at room temperature for 1 h before adjusting the pH to 2.0 by drop-wise adding 1 mol/L HCl. Pepsin was added to a final concentration of 1 mg/mL and the mixture was incubated on a shaker (95 rpm, Model 2314, Barnstead international, IA, USA) at 37 °C for 1 h. After gastric digestion, 0.9 mol/L sodium bicarbonate solution was added to the sample to raise the pH to 5.3. Next, pancreatin and bile extract was added to the solution and reached final concentrations of 0.4 and 2.4 mg/mL, respectively. The pH was then increased to 7.4 by the addition of 1 mol/L NaOH followed by incubating the mixture on a shaker (95 rpm) at 37 °C for a further 2.5 h. The reaction was terminated by boiling the solution for 5 min in water bath. Sample vials were blanketed with nitrogen at all incubation stages to avoid oxidation. Samples obtained from this process were referred as BC-NP digesta.

Caco-2 cells were seeded onto 12-well polyester clear Transwell® inserts (pore size 3 µm) at 2.6×10^5 cells/cm^2 [26]. The medium in apical and basolateral compartments was changed every other day for at least 21 days to allow the cells to

differentiate and form a confluent monolayer. The integrity of the cell monolayer was measured by routinely monitoring the TEER using an epithelial tissue voltohmmeter (EVOM2, World Precision Instruments, Saratosa, FL, USA). Monolayers with TEER values higher than 500 Ω· cm^2 were used for transport study. On the day of experiment, Caco-2 cell monolayers were washed 3 times with HBSS and pre-incubated at 37 °C for 1 h to reach equilibrium. BC-NP digesta (0.5 mg/mL in HBSS) were applied to apical compartments and equivalent amount of free β-carotene in Tween 40 suspension was used as control[27]. HBSS in basolateral compartments was replaced with HBSS containing 0.5 mmol/L taurochlorate, 1.6 mmol/L oleic acid and 45 mmol/L glycerol[28]. After a 16 h incubation at 37 °C, solutions in apical and basolateral compartments were collected and the cells were removed from the inserts for β-carotene extraction.

Method for β-carotene extraction from solutions in apical and basolateral chamber was adopted from Barba et al.[29] and Alheme et al.[30] Briefly, samples were extracted twice with hexane/ethanol/acetone (*v*/*v*/*v* = 50/25/25). The supernatant was pooled and evaporated under nitrogen stream with β-carotene residue left in the vial. β-Carotene extraction from the cells was performed using the method described by Peng et al.[31] Cells were pipetted off the inserts, pelleted by spinning at 800 × *g* for 10 min at 4 °C, resuspended with 1 mL of PBS containing 0.5 g/L butylated hydroxytoluene (BHT) and 2% (*w*/*v*) pronase E, and incubated at 37 °C for 45 min. Then cells were lysed by adding 1 mL of ethanol containing 0.5 g/L BHT and 10 g/L sodium dodecyl sulfate (SDS). After cell lysis, β-carotene in solution was extracted with hexane/ethanol/acetone (*v*/*v*/*v* = 50/25/25) and dried. The extracted residues from all samples were dissolved in 300 μL acetonitrile/ethanol (*v*/*v* = 65/35) and analyzed using a high performance liquid chromatography (HPLC) system (1200 series, Agilent Technologies, Inc., Santa Clara, CA, USA)[16]. Separation was carried out on a C18 column (150 mm × 4.6 mm, 2.6 μm, Kenitex, Phenomenex, Inc., Torrance, CA, USA) with a mobile phase of acetonitrile/ethanol (65:35, *v*/*v*) at the flow rate of 1 mL/min. β-Carotene was measured at the wavelength of 450 nm and quantified employing an external calibration. The transport efficiency was expressed as the amount of β-carotene in the basolateral media (ng) for unit area (cm^2) of Caco-2 cell monolayer.

2.9. *Ex vivo intestinal transport of nanoparticles using rat jejunum*

The animal care and experimental procedures were conducted in accordance with Canadian Council on Animal Care and approved by the University of Alberta Animal Care and Use Committee (Livestock). The *ex vivo* study was performed on a modified Ussing chamber model[32]. Male 10-week old Sprague–Dawley rats were purchased from Charles River Laboratories (Wilmington, MA, USA) and given free access to food and water. On the day of experiment, animals were anesthetized with isoflurance–oxygen mix (3.5%) and euthanized by exsanguination. The jejunum was removed distal to the ligament of the Treitz and immediately placed in ice-cold Krebs buffer supplemented with sodium L-glutamate (4.9 mmol/L), disodium fumarate (5.4 mmol/L), sodium pyruvate (4.9 mmol/L) and D-glucose (11.5 mmol/L) and continuously bubbled with O_2/CO_2 (95%/5%). Individual segments were cut from the jejunum and mounted in modified Ussing chambers (Harvard Apparatus Inc, Holliston, MA, USA). Each mounted area available for permeation was 1.15 cm^2.

NR-NP digesta was prepared using the same method for BC-NP digesta in previous section and added to the mucosal chamber to a final concentration of 0.5 mg/mL. After incubating for 60 and 90 min, solutions from mucosal and serosal chambers were collected and tissues were carefully removed. A small piece was cut from each segment and immediately mounted in embedding medium (Lamb-OCT, Thermo Scientific) on dry ice. Upon frozen, tissue blocks were stored at –20 °C until cryosection. Tissues were mounted on glass slides using Prolong® Gold Anitfade reagent without staining and examined with CLSM.

Solutions from each chamber were used to extract total lipid for Nile red quantification. Hexane/ethanol/acetone (50:25:25, *v*/*v*/*v*) was added to all solutions followed by centrifuge at 10,000 × *g* for 15 min. The hexane supernatant was pooled and dried under nitrogen stream. The residue was redissolved in 300 μL methanol and measured by SpectraMax M3 microplate reader (Molecular Devices, Sunnyvale, CA, USA) with the excitation and emission wavelength at 552 and 636 nm for Nile red fluorescence intensity. A standard curve indicating the quantitative relationship between Nile red intensity and NR-NP concentration was created by linear regression ($R^2 = 0.9994$). The standard was used to estimate the NR-NP digesta concentration in each chamber. The permeation was expressed as the amount of NR-NPs (μg) in the serosal side for unit area (cm^2) of jejunum tissue.

2.10. *Statistical analysis*

Data were expressed as mean ± SEM. Student's *t*-test was used for comparisons between two samples. The significant level was set as $P < 0.05$. Statistical analyses were performed using SAS 9.0 for Windows (SAS Institute Inc., Cary, NC, USA).

3. Results and discussion

3.1. *Characterization of nanoparticles from in vitro digestion of microparticles*

One of the most challenging issues in protein based oral delivery systems is their instability in gastric environment. A low pH environment and pepsin can denature and degrade protein nanoparticles, leading to burst leakage of encapsulated compounds in the stomach before reaching the small intestine, where most of drug/nutraceutical are absorbed. Barley protein microparticles were also digestible under pepsin proteolysis. However,

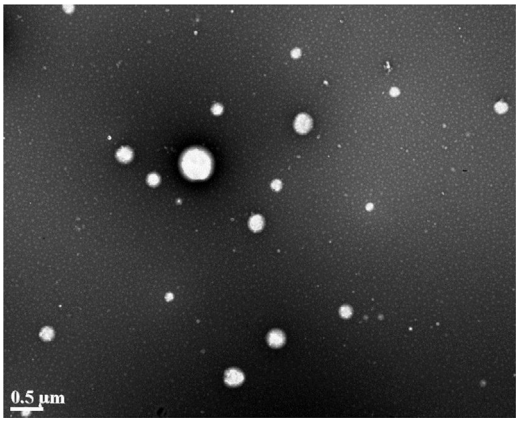

Figure 1 TEM micrographs of barley protein nanoparticles.

nanoparticles liberated from microparticles showed much improved stability in stomach. B-hordein was the major fraction stabilizing liberated nanoparticles after peptic digestion[11]. Pressure treatment can enhance the intermolecular β-sheets in B-hordein, resulting in solid interfacial network that could better stabilize nanoparticles in gastric environment than other proteins[33]. Meanwhile, major hydrophobic sections of B-hordein are protected under the compact interfacial network. This changes make B-hordein less vulnerable under the enzymatic hydrolysis from pepsin, which prefers to attack a hydrophobic/aromatic residue of protein[34].

In this study, nanoparticles were prepared by digesting microparticles with pepsin in a simulated gastric environment, rather than *de novo* synthesis using B-hordein. This was intended to mimic a natural digestion process, which allowed us to better understand the characteristics of nanoparticles in gastrointestinal track after being liberated from microparticles. The digestion process can also make the result from *in vitro* evaluation of nanoparticles more correlated with their *in vivo* performance. The β-carotene-loaded nanoparticles had an encapsulation efficiency of $90.7 \pm 1.4\%$ and a loading capacity of $0.069 \pm 0.001\%$. The dynamic light scattering results showed that nanoparticles had an average size of 351 ± 4 nm and zeta potential of -19.2 ± 1.9 mV. The polydispersity index (PdI) of nanoparticles was 0.33 ± 0.04, indicating relatively heterogeneous size distribution. The TEM image of obtained nanoparticles was shown in Fig. 1. Nanoparticles are spherical in shape and most of them have a size around 200 to 300 nm in diameter, although larger (500 nm) or smaller (50 nm) nanoparticle were also observed. This was in correspondence with the particle size variety observed in dynamic light scattering. The formation of nanoparticles was resulting from unrestricted proteolytic reaction of the protein matrix of microparticles, which made particle size hard be precisely controlled. Increasing the amount of B-hordein in microparticle preparation might be a strategy to obtain nanoparticles with better defined size, as it decreased the effect of proteolysis on formation of nanoparticles. However, this needs to be proven in the future experiment.

3.2. *Cytotoxicity of nanoparticles*

The cytotoxicity of BNPs was examined by FDA/PI staining. FDA can be taken up by live cells and hydrolyzed into the green fluorescent metabolite by intracellular esterase. While PI only passes through damaged cell membrane and intercalates with DNA/RNA, resulting in red fluorescence in injured or dead cells[21]. Compared to cells without BNPs exposure (control group), more than 80% cells were viable throughout 20 h exposure at a BNP concentration of 0.4 mg/mL and over 90% viability was observed at a BNP concentration range of 0.02–0.2 mg/mL (Fig. 2). Therefore, BNPs concentration of 0.2 mg/mL or lower was used in the following cell studies.

3.3. *Cellular internalization and localization of nanoparticles*

Efficient cellular uptake and sufficient retention time within cells is essential for nanoparticles as oral drug delivery systems[35]. In order to visualize and quantify the cellular uptake of nanoparticles, Nile red was incorporated in BNPs as fluorescent indicator (NR-NPs). The effects of incubation times, particle concentrations, and experimental temperatures on the nanoparticle uptake were investigated. Fig. 3A–C showed that at fixed nanoparticle concentration and experiment temperature (0.2 mg/mL, 37 °C), the fluorescent intensity in cells increased gradually at 0.5, 2 and 6 h, suggesting the uptake of nanoparticles was time dependant. This was also confirmed by result from flow cytometry (Fig. 4A). Moreover, the uptake of nanoparticles was found positively correlated to nanoparticle concentration. Under the same time and temperature condition, an increase of mean fluorescence intensity (MFI) in cell was observed when nanoparticle concentration increased from

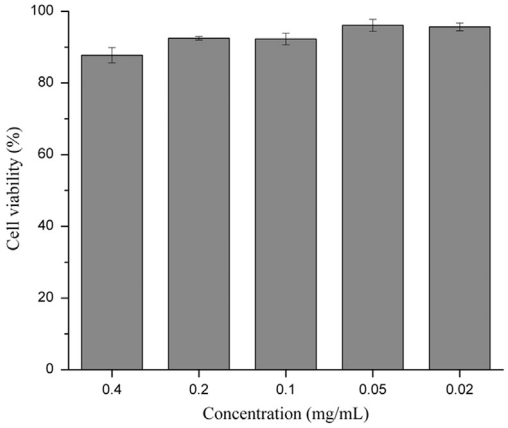

Figure 2 Cell viability of Caco-2 cells after incubation with barley protein nanoparticles for 20 h. Viability was presented by a percentage of living cells as a ratio of the living cells in the control group (without nanoparticles). Data are presented as mean ± SEM, $n = 3$.

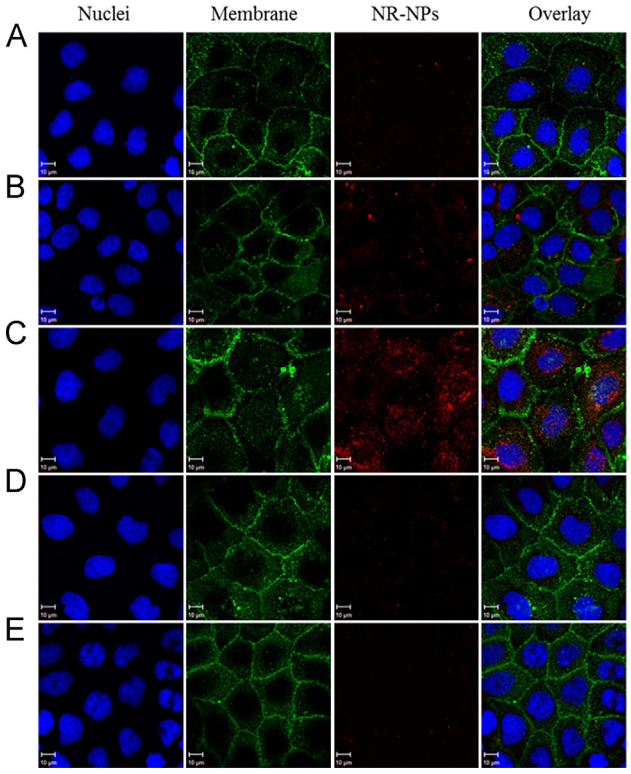

Figure 3 Confocal microscopic images of Caco-2 cells incubated with Nile red-labeled barley protein nanoparticles for different incubation times, at different concentrations and temperatures. (A) 0.5 h, 0.2 mg/mL, 37 °C; (B) 2 h, 0.2 mg/mL, 37 °C; (C) 6 h, 0.2 mg/mL, 37 °C; (D) 6 h, 0.02 mg/mL, 37 °C; (E) 6 h, 0.2 mg/mL, 4 °C. Red: NR-NPs, green: cell membrane, blue: nucleus.

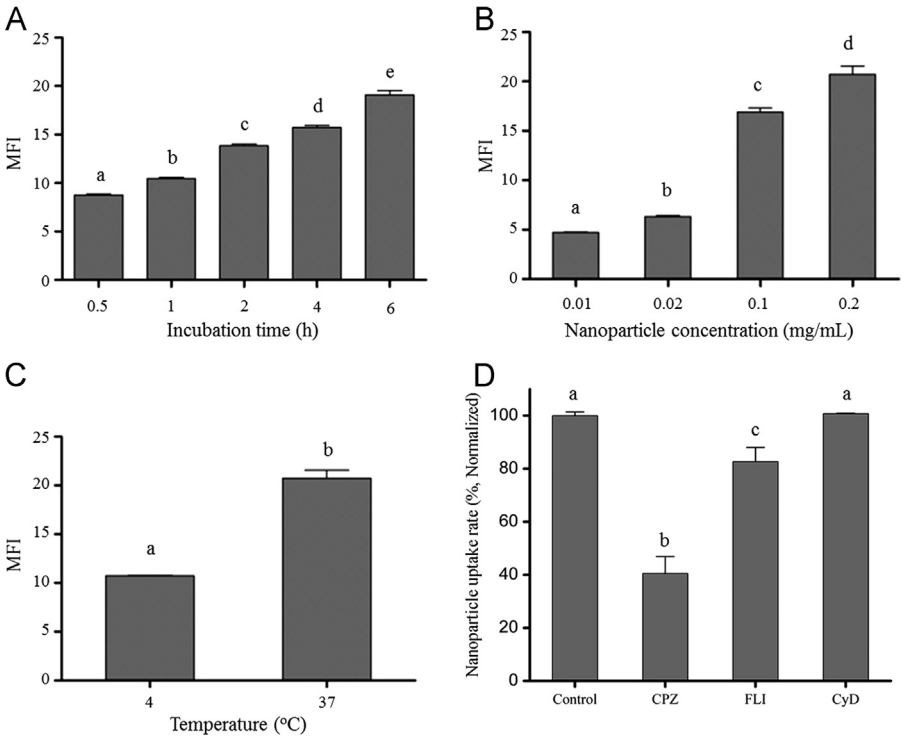

Figure 4 Flow cytometry analysis of cellular uptake of Nile red-labeled barley protein nanoparticles by Caco-2 cells, showing the effect of incubation time (A), nanoparticle concentration (B) and temperature (C). Endocytosis inhibition effect of different chemicals at 2 h (D): chlorpromazine hydrochloride (CPZ), filipin III (FLI) and cytochalasin D (CyD). Different letters indicate significant difference ($P<0.05$). MFI: mean fluorescence intensity. Data were presented as mean ± SEM, $n=3$.

0.01 to 0.2 mg/mL (Fig. 4B). Similarly, in CLSM, cells incubated with NR-NPs at 0.2 mg/mL exhibited stronger intracellular fluorescence signal than those incubated with NR-NP at lower contraction (0.02 mg/mL, Fig. 3C and D). Apart from incubation time and nanoparticle concentration, NR-NPs uptake was also affected by temperature. Low temperature could interfere with the synthesis and utilization of ATP in cell[36], which inhibit the energy dependent cellular uptake of nanoparticles[37]. When incubation was performed at 4 °C, nanoparticle uptake decreased by 51.7% compared to that at 37 °C (Fig. 4C). And barely any red fluorescence was observed in cells under CLSM at 4 °C (Fig. 3E). These results indicated the uptake of nanoparticles was energy dependent. There are three major energy dependent endocytic pathways for nanoparticle internalization: clathrin-mediated endocytosis (CME), caveolae-mediated endocytosis (CvME), and macropinocytosis[37]. In order to explore the uptake mechanism, CPZ, FLI, and CyD were used to inhibit CME, CvME and macropinocytosis, respectively[24,37]. As shown in Fig. 4D, the uptake efficiency decreased to 40.5% and 82.6% after CPZ and FLI treatments, respectively, while that with CyD treatment was not affected. These results suggested that the internalization of nanoparticles relied on both CME and CvME, with CME playing a more important role in the cellular uptake of BNPs.

On the other hand, both CME ($\leq$ 200 nm) and CvME (50–80 nm) have smaller cargo size than macropinocytosis (up to several micrometers)[38–40], suggesting both of these endocytic pathways are more likely to be involved in the transport of small particulates. In our scenario, BNPs liberated from microparticles had an average size of 351 nm, with smaller (50 nm) and large nanoparticles (500 nm) observed under TEM (Fig. 1). Considering the cargo size of CME and CvME, it could be expected that the nanoparticles with smaller size could enter the cells more efficiently than those with larger size.

Confocal microscopic image with three dimensional projections of Caco-2 cells after 6 h incubation with NR-NPs with a final concentration of 0.2 mg/mL at 37 °C was shown in Fig. 5. Although most NR-NPs were present in cytoplasm and accumulated around the nuclei, some nanoparticles were found within nuclei. The capability of nucleus internalization suggested barley protein nanoparticles had potential to be used as a delivery system in gene therapy, which requires further investigation.

3.4. *In vitro transport study*

In previous sections, nanoparticles with short gastric digestion were used for preliminary cell uptake study. However, in reality, nanoparticles would undergo pancreatic digestion and gradually degraded after reaching small intestine[11]. In order to better simulate the *in vivo* condition in small intestine, nanoparticles received extra digestion using pancreatin and bile extract before their transport efficiency were assessed. Chymotrypsin and trypsin are two major proteases in the pancreatin. In previous study, we found that barley protein nanoparticles could resist the digestion of chymotrypsin[24]. Similar to pepsin, chymotrypsin prefers to attack bulky hydrophobic amino acids[41]. After high pressure treatment, barley protein had hydrophobic groups hidden in the compact interfacial network, which made nanoparticles less vulnerable to chymotrypsin digestion. The barley protein coating could be hydrolyzed by trypsin, but the hydrolyzing process was relatively slow[7,24]. Hordein has very low lysine (~0%) and arginine (~2.7%) content[42,43], which are the exclusive target amino acids for trypsin[44]. Moreover, high proline (~21%) in hordein limits rotation of the prolyl peptide bond, making the formation of

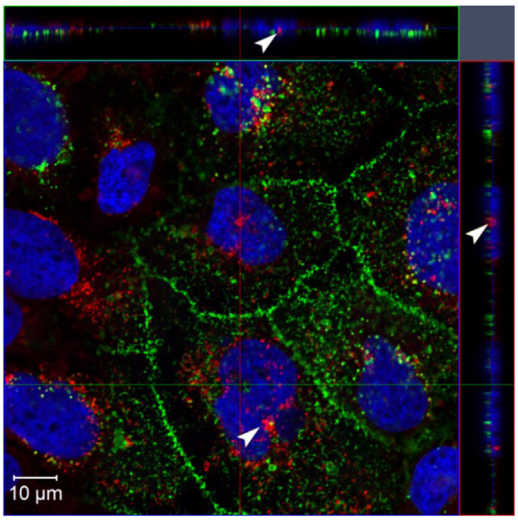

Figure 5 Confocal microscopic image of Caco-2 cells after 6 h incubation with Nile red-labeled barley protein nanoparticles (0.2 mg/mL) at 37 °C, presenting three-dimensional analysis of the optical *xy*-section (center square) with *xz*- and *yz*- projections (side panels). Image shows distinct uptake of nanoparticles by the cells; arrows heads indicate the presence of the nanoparticles within nuclei. Red: Nile red-labeled barley protein nanoparticles; green: cell membrane; blue: nuclei.

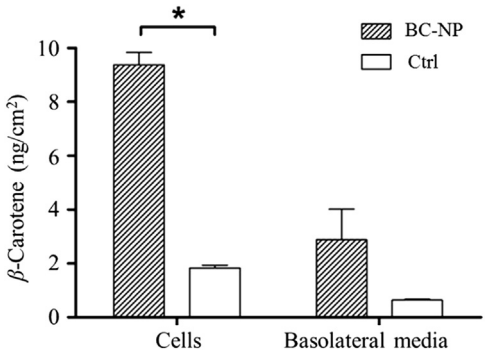

Figure 6 Uptake and transport of β-carotene in Caco-2 cell monolayers after 16 h incubation. Star shows significant difference compared to control ($P<0.05$). Data are presented as mean ± SEM, $n=2$. BC-NP: β-carotene-loaded barley protein nanoparticles; Ctrl: control, β-carotene in Tween 40 suspension.

geometric complimentary structure in protein that can fit the active site of trypsin more difficult[42,45]. β-Carotene was used as a model of hydrophobic compounds to indicate the transport efficacy of nanoparticle digesta. Addition of taurocholate and oleic acid allows Caco-2 cell monolayers to produce chylomicrons, which can incorporate β-carotene and excrete it to the basolateral side[46].

The uptake and transport of β-carotene in Caco-2 cell monolayers after 16 h incubation was represented in Fig. 6. When delivered by nanoparticle digesta, the β-carotene in cells was found at a concentration 9.38 ± 0.46 ng/cm^2 monolayer, accounting for $11.45 \pm 0.57\%$ of the total β-carotene applied to the apical chambers. This was significantly higher than those in control group (2.88 ± 1.14 ng/cm^2, $1.97 \pm 0.11\%$). Low solubility is the major barrier to prevent β-carotene from absorption. β-Carotene is not bioaccessible until being incorporated into micelles in intestine[47]. After barley protein nanoparticle encapsulation, β-carotene could be well dispersed in water and readily for intestinal absorption. Active cellular uptake of nanoparticles also contributed to the higher β-carotene concentration in cells. Although barley protein microencapsulation could effectively protect encapsulated compounds from degradation[10] and the *in situ* synthesis of nanoparticles from microparticles in stomach further prevent nanoparticles from aggregation and degradation during storage, the nanoparticles obtained from peptic digestion demonstrated relatively broad size distribution (50–500 nm). The size is a key factor for cellular uptake of nanoparticles. Smaller nanoparticles have a larger surface area-to-volume ratio which favors the interfacial interaction with cell membrane and the intracellular uptake of nanoparticles through intestinal epithelium[20]. Researches found that nanoparticles with diameter at around 50–200 nm were optimal for cellular uptake[9,35,48]. The uptake mechanism study in previous section also suggested that smaller nanoparticles were more likely to enter Caco-2 cells through endocytosis pathways. Therefore, liberated nanoparticles with smaller size (≤ 200 nm) should be considered as an important reason of the higher β-carotene concentration in cell monolayers. Surface hydrophobicity is another factor that modulates the internalization rates of nanoparticles. Increased nanoparticle surface hydrophobicity is favorable for the cellular uptake of nanoparticles[49], because hydrophobic surface made nanoparticles easily enter and stay in the hydrophobic domain of cell membrane[40]. In liberated nanoparticles, over 50% of protein coating were composed of nonpolar amino acids[11]. High nonpolar amino acid composition made the nanoparticle surface hydrophobic, which facilitated the internalization of nanoparticles.

The physiological absorption of β-carotene is a transcellular process[50] and the transport of β-carotene by nanoparticles across the Caco-2 monolayer could also follow the transcellular pathway, based on the evidences that nanoparticles actively internalized into cells through endocytosis and no significant change in TEER was observed before and after the transport study (data not shown). In basolateral chambers, β-carotene found in nanoparticle group (1.84 ± 0.10 ng/cm^2, $3.52 \pm 1.39\%$) was higher than that in control group (0.64 ± 0.04 ng/cm^2, $0.68 \pm 0.04\%$), but the difference was not significant. The rate of β-carotene secretion to the basolateral side is a transporter dependent and saturable process[51]. In nanoparticle group, much higher β-carotene content was found in cells, which might saturate the transporter and lead to reduced secretion to basolateral chamber.

3.5. *Ex vivo intestinal transport study*

The transport of nanoparticle digesta was further studied on an *ex vivo* rat intestine model using Ussing chamber technique. The *ex vivo* rat intestine model can better evaluate the transport efficiency of nanoparticles because it overcomes many shortcomings associated with Caco-2 cell monolayers, such as lack of intact intestinal structure (*e.g.*, mucosal layer) and lower expression of many transport proteins and metabolic enzymes[52]. Although β-carotene can be absorbed throughout the small intestine, duodenum and jejunum are considered as the major sites for β-carotene absorption[50,53–55]. Nanoparticles could enter enterocytes through non-specific endocytosis therefore their absorption was not restricted by the sections of the small intestine. However, because jejunum and ileum are much longer than duodenum, the absorption of nanoparticles is more likely to occur in the jejunum and ileum. Therefore, considering the absorption sites of both β-carotene and nanoparticles, jejunum was selected in

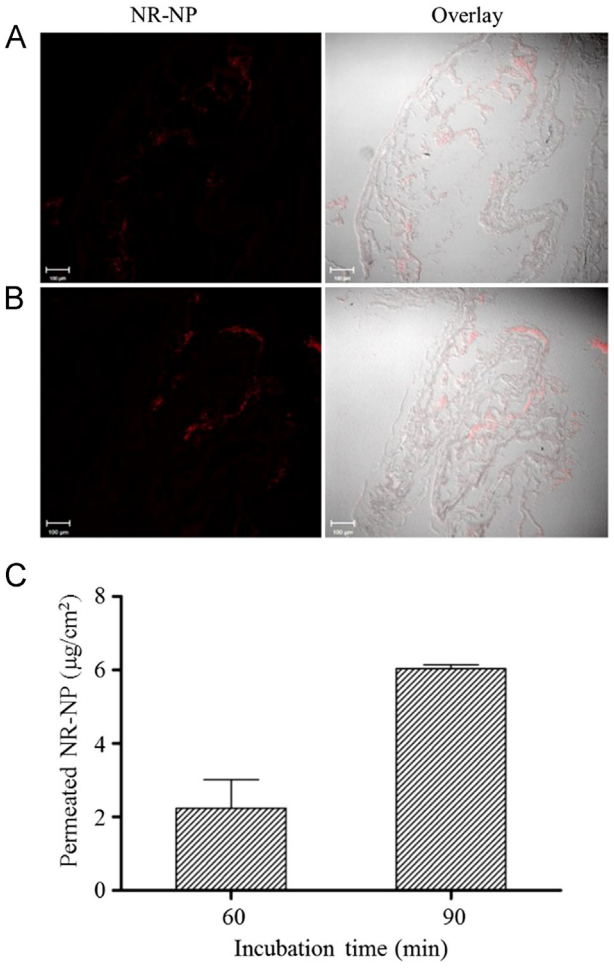

Figure 7 Confocal images of rat jejunum tissues incubated with digested Nile red-labeled barley protein nanoparticles for 60 min (A) and 90 min (B). Permeation of Nile red-labeled barley protein nanoparticles across rat jejunum in Ussing chambers (C). Data are presented as mean ± SEM, $n = 2$. NR-NP: Nile red-labeled barley protein nanoparticles.

the Ussing chamber study. After incubated with the digesta of NR-NPs for 60 and 90 min, red fluorescence was observed in intestinal tissues (Fig. 7A and B), suggesting nanoparticles were permeable to intestinal epithelia. The fluorescent intensity in tissues with 90 min incubation was stronger than that with 60 min incubation, indicating the intestinal uptake of nanoparticles was time dependent. This is consistent with uptake of nanoparticle in Caco-2 cell model (Fig. 4A). More importantly, the permeation of nanoparticle digesta also increased with time, reaching 2.24 ± 1.10 μg/cm^2 at 60 min and 6.04 ± 0.14 μg/cm^2 at 90 min (Fig. 7C), accounting for $0.17 \pm 0.08\%$ and $0.46 \pm 0.01\%$ of the total NR-NP digesta added to the mucosal chamber, respectively. These values were lower than that observed in Caco-2 monolayer transport study. The existence of mucosal network on epithelium may explain the difference. Protein nanoparticles with high hydrophobicity were able to efficiently adhere to mucosal network *via* hydrophobic interaction and hydrogen bonding[8]. The mucoadhesive property allows nanoparticles to resist the self-cleaning mechanisms of mucosal tissues and slow down their transit in intestine[56], which in turn increases intestinal resident time of nanoparticles and the encapsulated compounds. However, this property can also restrict the diffusion of nanoparticles across the mucosal network and decrease the contact between nanoparticles and intestinal epithelium[57,58]. Future research is required to balance the mucoadhesive property and transcellular efficiency and allow nanoparticles to reach optimal bioavailability.

4. Conclusions

This research investigated the biological effect of nanoparticles that were liberated from microparticles after an *in vitro* digestion. BNPs had an average size of 351 nm and PdI of 0.33. The particles showed low cytotoxicity on Caco-2 cells; more than 90% cells remained viable with exposure to BNPs for up to 20 h when nanoparticle concentration was lower than 0.2 mg/mL. CLSM showed BNPs were capable of travelling across cell membrane and entering Caco-2 cells. Quantitative study by flow cytometry demonstrated that the uptake process was particle concentration-, incubation time- and temperature-dependent. When β-carotene encapsulated nanoparticle digesta was delivered to Caco-2 cell monolayers, around 15% of total β-carotene was taken up into and transported across the cells, which was significantly higher than β-carotene without nanoparticle carriers. In *ex vivo* intestinal permeability study, approximately 0.17% and 0.46% nanoparticle digesta was able to permeate through intestinal tissue and translocated to the serosal side after 60 and 90 min respectively. Overall, this study shows the great potential of BNPs in enhancing bioavailability of lipophilic compounds after oral administration.

Acknowledgments

The authors are grateful to the Natural Sciences and Engineering Research Council of Canada (NSERC), Alberta Crop Industry Development Fund Ltd. (ACIDF), Alberta Innovates Bio Solutions (AI Bio) and Alberta Barley Commission for their funding support. Dr. Lingyun Chen would like to thank the Natural Sciences and Engineering Research Council of Canada (NSERC)-Canada Research Chairs Program for its financial support.

References

1. Zhu L, Lu L, Wang S, Wu J, Shi J, Yan T, et al. Oral absorption basics: pathways and physicochemical and biological factors affecting absorption. In: Chen Y, Zhang GG, Yu L, Mantri RV, editors. *Developing solid oral dosage forms*. 2nd ed. Boston: Academic Press; 2017. p. 297–329.
2. Shekhawat PB, Pokharkar VB. Understanding peroral absorption: regulatory aspects and contemporary approaches to tackling solubility and permeability hurdles. *Acta Pharm Sin B* 2017;**7**:260–80.
3. Berardi A, Bisharat L. Nanotechnology systems for oral drug delivery: challenges and opportunities. In: Massadeh S, editor. *Nanotechnology in drug delivery*. Cheshire: One Central Press; 2014. p. 53–74.
4. Chen L, Remondetto GE, Subirade M. Food protein-based materials as nutraceutical delivery systems. *Trends Food Sci Technol* 2006;**17**:272–83.
5. Tarhini M, Greige-Gerges H, Elaissari A. Protein-based nanoparticles: from preparation to encapsulation of active molecules. *Int J Pharm* 2017;**522**:172–97.
6. Zhang Y, Sun T, Jiang C. Biomacromolecules as carriers in drug delivery and tissue engineering. *Acta Pharm Sin B* 2018;**8**:34–50.
7. Yang J, Zhou Y, Chen L. Elaboration and characterization of barley protein nanoparticles as an oral delivery system for lipophilic bioactive compounds. *Food Funct* 2014;**5**:92–101.

8. Arangoa MA, Ponchel G, Orecchioni AM, Renedo MJ, Duchêne D, Irache JM. Bioadhesive potential of gliadin nanoparticulate systems. *Eur J Pharm Sci* 2000;**11**:333–41.
9. Zhang J, Field CJ, Vine D, Chen L. Intestinal uptake and transport of vitamin B12-loaded soy protein nanoparticles. *Pharm Res* 2015;**32**:1288–303.
10. Wang R, Tian Z, Chen L. A novel process for microencapsulation of fish oil with barley protein. *Food Res Int* 2011;**44**:2735–41.
11. Wang R, Tian Z, Chen L. Nano-encapsulations liberated from barley protein microparticles for oral delivery of bioactive compounds. *Int J Pharm* 2011;**406**:153–62.
12. Xu P, Gullotti E, Tong L, Highley CB, Errabelli DR, Hasan T, et al. Intracellular drug delivery by poly(lactic-*co*-glycolic acid) nanoparticles, revisited. *Mol Pharm* 2009;**6**:190–201.
13. Li Q, Li C, Tong W. Nile red loaded PLGA nanoparticles surface modified with Gd-DTPA for potential dual-modal imaging. *J Nanosci Nanotechnol* 2016;**16**:5569–76.
14. Roger E, Lagarce F, Garcion E, Benoit JP. Lipid nanocarriers improve paclitaxel transport throughout human intestinal epithelial cells by using vesicle-mediated transcytosis. *J Control Release* 2009;**140**:174–81.
15. Aksungur P, Demirbilek M, Denkbaş E, Ünlü N. Comparative evaluation of cyclosporine A/HPβCD-incorporated PLGA nanoparticles for development of effective ocular preparations. *J Microencapsul* 2012;**29**:605–13.
16. Wang P, Liu HJ, Mei XY, Nakajima M, Yin LJ. Preliminary study into the factors modulating β-carotene micelle formation in dispersions using an *in vitro* digestion model. *Food Hydrocoll* 2012;**26**:427–33.
17. Gul K, Tak A, Singh AK, Singh P, Yousuf B, Wani AA. Chemistry, encapsulation, and health benefits of β-carotene—a review. *Cogent Food Agric* 2015;**1**:1018696.
18. Liang R, Shoemaker CF, Yang X, Zhong F, Huang Q. Stability and bioaccessibility of β-carotene in nanoemulsions stabilized by modified starches. *J Agric Food Chem* 2013;**61**:1249–57.
19. Cornwell DG, Kruger FA, Robinson HB. Studies on the absorption of β-carotene and the distribution of total carotenoid in human serum lipoproteins after oral administration. *J Lipid Res* 1962;**3**:65–70.
20. Harde H, Das M, Jain S. Solid lipid nanoparticles: an oral bioavailability enhancer vehicle. *Expert Opin Drug Deliv* 2011;**8**:1407–24.
21. Jones KH, Senft JA. An improved method to determine cell viability by simultaneous staining with fluorescein diacetate–propidium iodide. *J Histochem Cytochem* 1985;**33**:77–9.
22. Chen K, Gunter K, Maines MD. Neurons overexpressing heme oxygenase-1 resist oxidative stress-mediated cell death. *J Neurochem* 2000;**75**:304–13.
23. Huang W, Wang Y, Chen Y, Zhao Y, Zhang Q, Zheng X, et al. Strong and rapidly self-healing hydrogels: potential hemostatic materials. *Adv Healthc Mater* 2016;**5**:2813–22.
24. Liu G, Huang W, Babii O, Gong X, Tian Z, Yang J, et al. Novel protein–lipid composite nanoparticles with an inner aqueous compartment as delivery systems of hydrophilic nutraceutical compounds. *Nanoscale* 2018;**10**:10629–40.
25. Garrett DA, Failla ML, Sarama RJ. Development of an *in vitro* digestion method to assess carotenoid bioavailability from meals. *J Agric Food Chem* 1999;**47**:4301–9.
26. Hubatsch I, Ragnarsson EGE, Artursson P. Determination of drug permeability and prediction of drug absorption in Caco-2 monolayers. *Nat Protoc* 2007;**2**:2111–9.
27. During A, Albaugh G, Smith Jr JC. Characterization of β-carotene 15,15′-dioxygenase activity in TC7 clone of human intestinal cell line Caco-2. *Biochem Biophys Res Commun* 1998;**249**:467–74.
28. Netzel M, Netzel G, Zabaras D, Lundin L, Day L, Addepalli R, et al. Release and absorption of carotenes from processed carrots (*Daucus carota*) using *in vitro* digestion coupled with a Caco-2 cell trans-well culture model. *Food Res Int* 2011;**44**:868–74.
29. Barba AI, Hurtado MC, Mata MC, Ruiz VF, de Tejada ML. Application of a UV–Vis detection-HPLC method for a rapid determination of lycopene and β-carotene in vegetables. *Food Chem* 2006;**95**:328–36.
30. Aherne SA, Daly T, Jiwan MA, O'Sullivan L, O'Brien NM. Bioavailability of β-carotene isomers from raw and cooked carrots using an *in vitro* digestion model coupled with a human intestinal Caco-2 cell model. *Food Res Int* 2010;**43**:1449–54.
31. Peng YM, Peng YS, Lin Y, Moon T, Roe DJ, Ritenbaugh C. Concentrations and plasma–tissue–diet relationships of carotenoids, retinoids, and tocopherols in humans. *Nutr Cancer* 1995;**23**:233–46.
32. Vine DF, Charman SA, Gibson PR, Sinclair AJ, Porter CJ. Effect of dietary fatty acids on the intestinal permeability of marker drug compounds in excised rat jejunum. *J Pharm Pharmacol* 2002;**54**:809–19.
33. Yang J, Huang J, Zeng H, Chen L. Surface pressure affects B-hordein network formation at the air–water interface in relation to gastric digestibility. *Colloids Surf B* 2015;**135**:784–92.
34. Kageyama H, Ueda H, Tezuka T, Ogasawara A, Narita Y, Kageyama T, et al. Differences in the P1′ substrate specificities of pepsin A and chymosin. *J Biochem* 2010;**147**:167–74.
35. Win KY, Feng SS. Effects of particle size and surface coating on cellular uptake of polymeric nanoparticles for oral delivery of anticancer drugs. *Biomaterials* 2005;**26**:2713–22.
36. Negendank W, Shaller C. Temperature-dependence of ATP level, organic phosphate production and Na,K-ATPase in human lymphocytes. *Physiol Chem Phys* 1982;**14**:513–8.
37. Xiang S, Tong H, Shi Q, Fernandes JC, Jin T, Dai K, et al. Uptake mechanisms of non-viral gene delivery. *J Control Release* 2012;**158**:371–8.
38. Conner SD, Schmid SL. Regulated portals of entry into the cell. *Nature* 2003;**422**:37–44.
39. Iversen TG, Skotland T, Sandvig K. Endocytosis and intracellular transport of nanoparticles: present knowledge and need for future studies. *Nano Today* 2011;**6**:176–85.
40. Behzadi S, Serpooshan V, Tao W, Hamaly MA, Alkawareek MY, Dreaden EC, et al. Cellular uptake of nanoparticles: journey inside the cell. *Chem Soc Rev* 2017;**46**:4218–44.
41. Appel W. Chymotrypsin: molecular and catalytic properties. *Clin Biochem* 1986;**19**:317–22.
42. Wang C, Tian Z, Chen L, Temelli F, Liu H, Wang Y. Functionality of barley proteins extracted and fractionated by alkaline and alcohol methods. *Cereal Chem* 2010;**87**:597–606.
43. Qi JC, Chen JX, Wang JM, Wu FB, Cao LP, Zhang GP. Protein and hordein fraction content in barley seeds as affected by sowing date and their relations to malting quality. *J Zhejiang Univ Sci B* 2005;**6**:1069–75.
44. Olsen JV, Ong SE, Mann M. Trypsin cleaves exclusively C-terminal to arginine and lysine residues. *Mol Cell Proteom* 2004;**3**:608–14.
45. Simpson DJ. Proteolytic degradation of cereal prolamins—the problem with proline. *Plant Sci* 2001;**161**:825–38.
46. During A, Harrison EH. An *in vitro* model to study the intestinal absorption of carotenoids. *Food Res Int* 2005;**38**:1001–8.
47. Desmarchelier C, Borel P. Overview of carotenoid bioavailability determinants: from dietary factors to host genetic variations. *Trends Food Sci Technol* 2017;**69**:270–80.
48. Desai MP, Labhasetwar V, Walter E, Levy RJ, Amidon GL. The mechanism of uptake of biodegradable microparticles in Caco-2 cells is size dependent. *Pharm Res* 1997;**14**:1568–73.
49. Samadi Moghaddam M, Heiny M, Shastri VP. Enhanced cellular uptake of nanoparticles by increasing the hydrophobicity of poly(lactic acid) through copolymerization with cell-membrane-lipid components. *Chem Commun* 2015;**51**:14605–8.
50. Parker RS. Absorption, metabolism, and transport of carotenoids. *FASEB J* 1996;**10**:542–51.
51. During A, Hussain MM, Morel DW, Harrison EH. Carotenoid uptake and secretion by Caco-2 cells: β-carotene isomer selectivity and carotenoid interactions. *J Lipid Res* 2002;**43**:1086–95.
52. Lundquist P, Artursson P. Oral absorption of peptides and nanoparticles across the human intestine: opportunities, limitations and studies in human tissues. *Adv Drug Del Rev* 2016;**106**:256–76.

53. Hollander D, Ruble Jr PE. β-Carotene intestinal absorption: bile, fatty acid, pH, and flow rate effects on transport. *Am J Physiol* 1978;**235**:E686–91.
54. Wang XD, Russell RM, Marini RP, Tang G, Dolnikowski GG, Fox JG, et al. Intestinal perfusion of β-carotene in the ferret raises retinoic acid level in portal blood. *Biochim Biophys Acta* 1993;**1167**:159–64.
55. Goncalves A, Roi S, Nowicki M, Dhaussy A, Huertas A, Amiot MJ, et al. Fat-soluble vitamin intestinal absorption: absorption sites in the intestine and interactions for absorption. *Food Chem* 2015;**172**:155–60.
56. das Neves J, Bahia MF, Amiji MM, Sarmento B. Mucoadhesive nanomedicines: characterization and modulation of mucoadhesion at the nanoscale. *Expert Opin Drug Deliv* 2011;**8**:1085–104.
57. Palazzo C, Trapani G, Ponchel G, Trapani A, Vauthier C. Mucoadhesive properties of low molecular weight chitosan- or glycol chitosan- and corresponding thiomer-coated poly(isobutylcyanoacrylate) core-shell nanoparticles. *Eur J Pharm Biopharm* 2017;**117**:315–23.
58. Laffleur F, Hintzen F, Shahnaz G, Rahmat D, Leithner K, Bernkop-Schnürch A. Development and *in vitro* evaluation of slippery nanoparticles for enhanced diffusion through native mucus. *Nanomedicine* 2014;**9**:387–96.